Waste Management 112 (2020) 40–51

Contents lists available at ScienceDirect

Waste Management

journal homepage: www.elsevier.com/locate/wasman

Estimating black soldier fly larvae biowaste conversion performance by simulation of midgut digestion

Moritz Gold [a,b], Julia Egger [a,b], Andreas Scheidegger [c], Christian Zurbrügg [b], Daniele Bruno [d], Marco Bonelli [e], Gianluca Tettamanti [d,h], Morena Casartelli [e,h], Eric Schmitt [f], Ben Kerkaert [g], Jeroen De Smet [g], Leen Van Campenhout [g], Alexander Mathys [a,*]

[a] ETH Zurich: Swiss Federal Institute of Technology Zurich, Institute of Food, Nutrition and Health, Sustainable Food Processing Laboratory, Schmelzbergstrasse 9, 8092 Zurich, Switzerland
[b] Eawag: Swiss Federal Institute of Aquatic Science and Technology, Department Sanitation, Water and Solid Waste for Development (Sandec), Überlandstrasse 133, 8600 Dübendorf, Switzerland
[c] Eawag: Swiss Federal Institute of Aquatic Science and Technology, Department Systems Analysis, Integrated Assessment and Modelling, Überlandstrasse 133, 8600 Dübendorf, Switzerland
[d] University of Insubria, Department of Biotechnology and Life Sciences, via J.H. Dunant 3, 21100, Varese, Italy
[e] University of Milan, Department of Biosciences, via G. Celoria 26, 20133, Milan, Italy
[f] Protix B.V., Industriestraat 3, 5107 NC, Dongen, the Netherlands
[g] KU Leuven, Department of Microbial and Molecular Systems (M2S), Lab4Food, Campus Geel, Kleinhoefstraat 4, 2440 Geel, Belgium
[h] Interuniversity Center for Studies on Bioinspired Agro-environmental Technology (BAT Center), University of Napoli Federico II, via Università 100, 80055 Portici, Italy

ARTICLE INFO

Article history:
Received 2 April 2020
Revised 15 May 2020
Accepted 16 May 2020

Keywords:
Feed
Bioconversion
Waste
Insect
Residence time
Hermetia illucens

ABSTRACT

Black soldier fly larvae treatment is an emerging technology for the conversion of biowaste into potentially more sustainable and marketable high-value products, according to circular economy principles. Unknown or variable performance for different biowastes is currently one challenge that prohibits the global technology up-scaling. This study describes simulated midgut digestion for black soldier fly larvae to estimate biowaste conversion performance. Before simulation, the unknown biowaste residence time in the three midgut regions was determined on three diets varying in protein and non-fiber carbohydrate content. For the static *in vitro* model, diet residence times of 15 min, 45 min, and 90 min were used for the anterior, middle, and posterior midgut region, respectively. The model was validated by comparing the ranking of diets based on *in vitro* digestion products to the ranking found in *in vivo* feeding experiments. Four artificial diets and five biowastes were digested using the model, and diet digestibility and supernatant nutrient contents were determined. This approach was able to distinguish broadly the worst and best performing rearing diets. However, for some of the diets, the performance estimated based on *in vitro* results did not match with the results of the feeding experiments. Future studies should try to establish a stronger correlation by considering fly larvae nutrient requirements, hemicellulose digestion, and the diet/gut microbiota. *In vitro* digestion models could be a powerful tool for academia and industry to increase conversion performance of biowastes with black soldier fly larvae.

1. Introduction

Black soldier fly larvae (BSFL), *Hermetia illucens* L. (Diptera: Stratiomyidae), treatment is an emerging technology for the conversion of biowaste (Dortmans et al., 2017) into marketable high-value products according to circular economy principles (Bortolini et al., 2020; Cappellozza et al., 2019; Leong et al., 2016; Setti et al., 2019; Vilcinskas, 2013; Wang and Shelomi, 2017). In addition to the recycling of nutrients into raw materials for fertilizer, lubricant and biodiesel, pharmaceutical, and animal

Abbreviations: AMG, Anterior midgut; BSFL, Black soldier fly larvae; DM, Dry mass; MMG, Middle midgut; NFC, Non-fiber carbohydrates; $P^{13}NFC^{8}$, artificial diet with 13% protein, 8% NFC and 76% fibres; $P^{13}NFC^{47}$, artificial diet with 13% protein, 47% NFC and 37% fibres; $P^{7}NFC^{47}$, artificial diet with 7% protein, 47% NFC and 42% fibres; $P^{7}NFC^{78}$, artificial diet with 7% protein, 78% NFC and 11% fibres; PMG, Posterior midgut; TN, Total nitrogen; TOC, Total organic carbon.

* Corresponding author.
E-mail address: alexander.mathys@hest.ethz.ch (A. Mathys).

https://doi.org/10.1016/j.wasman.2020.05.026
0956-053X/

feed markets, BSFL treatment can have environmental benefits. For example, depending on the operational conditions, BSFL conversion can reduce emissions from biowaste treatment in comparison to composting (Ermolaev et al., 2019; Mertenat et al., 2019; Pang et al., 2020), and animal feed products can have a lower environmental impacts than conventional feeds when produced with BSFL (Smetana et al., 2019, 2016).

One current challenge for the replication and up-scaling of BSFL biowaste treatment is the often unknown or variable treatment performance (Gold et al. 2020, Gold et al. 2018a). Metrics that correlate with treatment performance, similar to those determined for other biowaste treatment technologies, such as the biomethane potential for anaerobic digestion, and the carbon and nitrogen ratio for composting, are lacking for BSFL treatment, but could provide parameters for the reliable design and operation. Such metrics could be delivered by *in vitro* digestion models widely applied in research on humans (Brodkorb et al., 2019; Minekus et al., 2014) and farmed animals (Boisen and Eggum, 1991; Cheli et al., 2012; Fuller, 1991). Static *in vitro* digestion models are particularly popular and useful because of their simplicity, reproducibility, and low cost while still providing results predicting *in vivo* digestion outcomes (Bohn et al., 2018). They have been widely used to predict the quality and digestibility of animal diets with the goal of optimizing health and growth of farmed monogastric (e.g., poultry, pigs) and ruminant (e.g., cows) animals (Boisen and Fernández, 1997; Noblet and Jaguelin-Peyraud, 2007; Tilley and Terry, 1963; Van Soest, 1994). Simulation of digestion could have similar applications in BSFL treatment. Nutrient contents in products following *in vitro* digestion could be used to predict *in vivo* performance (e.g., larval growth, waste reduction) (Kiers et al., 2000; McClements et al., 2009; Oomen et al., 2002, 2003). Thereby, simulation of BSFL digestion may enable direct and cost-effective comparison of biowastes with different compositions (e.g., nutrient contents, microbial loads, textures, moisture contents, and bulk densities).

BSFL digestion could be mimicked in the laboratory by exposing diets to pH values, temperatures, enzyme activities, and residence times similar to those found in the digestive tract of BSFL (Brodkorb et al., 2019; Hur et al., 2011; McDonald et al., 2011; Minekus et al., 2014). As the digestive tract of fly larvae presents some similarities to that of humans (Bonelli et al., 2019; Gold et al. 2018a; Jiang et al., 2015), a starting point for the development of BSFL *in vitro* simulations could be the static human *in vitro* digestion model, for which an international standard method was recently proposed (Brodkorb et al., 2019). In addition, the knowledge on the BSFL biology should be considered. The midgut is the most important organ for digestion in insects (Caccia et al., 2019). The midgut in BSFL is divided into three regions, i.e., anterior midgut (AMG), middle midgut (MMG), and posterior midgut (PMG), each with its own peculiar morphofunctional features (Bonelli et al., 2019; Bruno et al., 2019). Therefore, the *in vitro* digestion model should mimic this organization. Bonelli et al. (2019) reported the pH values of the lumen in the different midgut regions, and the activity of the enzymes involved in protein, carbohydrate, and lipid digestion, with results being in line with fly larvae digestion (Gold et al. 2018a). Even though this information is crucial for developing a static *in vitro* digestion model, reliable information regarding residence times of biowaste in the three midgut regions is also indispensable and, thus far, is not available for BSFL.

The aim of this research was to implement and validate a static *in vitro* model of the BSFL midgut. Before *in vitro* digestions, diet residence time was determined as a missing input parameter. Digestion was simulated to assess whether nutrient contents in *in vitro* digestion products could be indicative of *in vivo* feeding experiment outcomes. Despite the simplicity of the model which mimics only one digestion and does not consider temperature dynamics, we hypothesized that *in vitro* diet digestibility and supernatant nutrient contents correlate with *in vivo* waste reduction and larval weight. Thereby, an *in vitro* model could be a powerful tool in academia and industry to increase the understanding and performance of the BSFL treatment process.

2. Materials and methods

This research consisted of four parts: i) Determination of diet residence times in the three midgut regions (section 2.1.); ii) *in vitro* simulation of BSFL digestion using the midgut region residence time estimates (section 2.2.); iii) *in vivo* feeding experiments (section 2.3.); and iv) comparison of *in vitro* and *in vivo* results (section 2.4.).

2.1. Determination of diet midgut residence times and diet intake

2.1.1. Artificial diets

Residence times of diet in the three midgut regions was determined as a missing input parameter for a static *in vitro* model mimicking BSFL digestion. Gut residence times have previously been shown to vary for many organism with the diet nutrient content (Karasov et al., 2011). To receive a representative estimate for *in vitro* simulation, midgut residence time was determined with three artificial diets varying in nutrient contents. The diets were similar to those previously used by Cammack and Tomberlin (2017) and had the same lipid, vitamin, and mineral content, but two different protein and three different NFC contents (Table 1, Table S1). Contents were selected to reflect the range of protein and NFC contents typical for BSFL substrates. The differences in protein and NFC were balanced with cellulose, which was mostly indigestible under the experimental conditions used in this study (Gold et al. 2018b). Protein:NFC:Fibre contents in % dry mass (DM) were 13:8:76, 13:47:37, and 7:47:42 in the artificial diets; henceforth, these diets are referred to as $P^{13}NFC^{8}$, $P^{13}NFC^{47}$ and $P^{7}NFC^{47}$, respectively. Based on preliminary experiments, the dry artificial diets were mixed with different amounts of water to account for different diet water adsorptions (Stana-Kleinschek et al., 2002) to 70% (for $P^{13}NFC^{47}$ and $P^{7}NFC^{47}$) and 80% (for $P^{13}NFC^{8}$) moisture content.

2.1.2. Dye

Residence times were determined by mixing the artificial diets with the dye Blue 1 (Deshpande et al., 2014; Espinoza-Fuentes and Terra, 1987; Kim et al., 2018; Rodrigues et al., 2015) and observing the foremost dye position (i.e., interface between artificial diet without blue dye and artificial diet with blue dye, see Fig. S1) over time via larval dissection. Preliminary experiments with poultry feed (UFA 625, UFA AG, Switzerland) confirmed that the effect of Blue 1 on larval weight and waste reduction was not significant (one-way ANOVA, $p < 0.05$).

2.1.3. Black soldier fly larvae (BSFL)

Larvae used in the experiments were from a BSFL research colony at Eawag. Eggs were placed for 24 h on commercial poultry feed (UFA 625, UFA AG, Switzerland). Afterwards, BSFL were fed *ad libitum* with poultry feed for 13 to 14 days. In the entire study, BSFL were separated from the diet/residue using sieves, washed with deionized water, and briefly dried using paper towels. As diet residence time can be expected to depend on organism life stage (Chapman, 2013; Edgecomb et al., 1994), following separation, larvae were used for determination of morphometric parameters. Larval weight (n = 75, n = total number of larvae) was determined with a precision balance (BM-65, Phoenix instrument, Germany). The length of the midgut regions (n = 10) and cephalic capsule

Table 1
Mean nutrient composition of diets used in this study.

	Protein	NFC	Lipids	Fiber	Organic matter	P:NFC* ratio
	% DM	% DM	% DM	% DM	% DM	–
Artificial diets						
$P^{13}NFC^{8}$	12.6	7.8	0.6	75.7	96.7	2:1
$P^{13}NFC^{47}$	12.6	46.8	0.6	36.7	96.7	1:4
$P^{7}NFC^{78}$	7.0	77.8	0.6	11.3	96.7	1:11
$P^{7}NFC^{47}$	7.0	46.7	0.6	42.4	96.7	1:7
Biowastes						
Cow manure	11.1 (0.4)	1.8 (0.6)	4.4	58.4 (0.4)	80.7 (0.5)	7:1
Mill by-products	14.5 (0.3)	23.2 (0.2)	3.0	51.7 (0.9)	93.8 (1.3)	1:2
Canteen waste	32.2 (0.8)	7.5 (0.7)	34.9	36.2 (1.4)	93.0 (0.7)	4:1
Poultry slaughterhouse waste	37.3 (0.5)	0.3 (0.1)	42.9	20.8 (1.9)	94.0 (1.3)	152:1
Vegetable canteen waste	12.1 (0.1)	15.5 (0.9)	28.9	31.5 (1.8)	92.4 (0.5)	1:1

In parenthesis: standard deviation for samples where n ≥ 3 and differences between analyses where n = 2.
Composition of artificial diets was calculated based on the proportion/composition of the artificial diet ingredients (see Table S1).
Composition of biowastes taken from Gold et al. (2020).
* P:NFC = protein to NFC.

width (n = 10) were determined via a stereomicroscope (SZX10, Olympus Corporation, Tokyo, Japan) and the corresponding image analysis software (cellSens Dimensions, Version 1.18, Olympus Corporation, Tokyo, Japan). The larval instar was determined using the cephalic capsule measurement and the classification proposed by Barros et al. (2018).

2.1.4. Feeding experiment

Since changing the diet from poultry feed to the artificial diets may influence the midgut residence time, larvae were placed for 24 h on the artificial diets containing no dye following separation from the poultry feed. The larvae were then separated from the artificial diets and placed into new containers with the respective artificial diets containing 0.05% (w/v) Blue 1. Three plastic containers (diameter: 7.1 cm, height: 11 cm) were prepared for each artificial diet containing 70 larvae (larval density: 1.8 larvae/cm^2) and 50 g artificial diet (wet weight). Subsequently, after 10 (only experiment two and three), 20, 40, 60, 90, 120, 150, and 180 min, 10 larvae were randomly removed from each colored artificial diet using tweezers. The larvae were separated from the diet/residue and directly placed at −20 °C. The experiment was replicated in singlets three times. All feeding experiments were performed without light in a climate chamber (HPP 266, Memmert GmbH, Germany, 28 °C, 70% relative humidity).

2.1.5. Visual determination of the foremost dye position

The foremost position of the dye (see Fig. S1) in the midgut was determined with a stereomicroscope (SZX10, Olympus Corporation, Tokyo, Japan) following dissection of the larvae. Directly before dissection, the larvae were removed from the freezer and kept on ice. For each diet, time point, and experiment, ten larvae were analyzed. The entire gut was removed from the frozen larvae, placed in phosphate buffered saline, and the fat body and trachea surrounding the gut were removed. To define the position of the dye along the midgut, the different regions of this organ (AMG, MMG, and PMG) were identified (see Fig. S1). To increase the resolution of diet residence time determination, PMG, which is the longest region of the midgut, was further subdivided into PMG1 and PMG2. This classification of the midgut into different regions followed the morphofunctional midgut characterization by Bonelli et al. (2019). Larvae that did not eat, or for which no clear allocation in the above mentioned regions was evident, were excluded from the analysis. These larvae accounted for 12.6% of total larvae dissected.

2.1.6. Modelling of diet midgut residence time distributions

The data on the foremost dye position in the midgut were used to model the midgut residence time distributions. The observation (t,j) from the dissection of individual BSFL provides the information that the diet has reached the j_{th} region at time t. The residence time in the i_{th} gut region, $i = 1 \cdots 4$, is represented by the random variable X_i with probability distribution $p_i(:;\theta_i)$ parametrized by θ_i. Assuming the residence times are independent, the total time for the diet to travel from the beginning until the end of the j_{th} midgut region is the sum of the corresponding residence times according to Equation (1). It is possible that diet residence times in gut regions are dependent on those of previous regions, but data of this study was insufficient to estimate these conditional probabilities.

$$T_j = \sum_{i=1}^{j} X_i \tag{1}$$

The probability distribution T_j, which is a random variable, was derived numerically by the R package distr (Ruckdeschel and Kohl, 2014) to construct the following survival functions:

$$\begin{aligned}&\text{Prob (at time } t \text{ that the diet has not yet passed region } j)\\ &= \text{Prob}(t < T_j) = S_j(t;\theta)\end{aligned} \tag{2}$$

where θ contains the (unknown) parameters of all the underlying residence time distributions. From equation (2), the likelihood function for a single observation (t,j) can be expressed as:

$$\text{Prob}((\text{t},\text{j})|\theta) = \text{Prob}(T_{j-1} < t \le T_j|\theta) = \begin{cases} S_1(t;\theta) & j = 1 \\ S_j(t;\theta) - S_{j-1}(t;\theta) & \text{else} \\ 1 - S_3(t;\theta) & j = 4 \end{cases} \tag{3}$$

Finally, the likelihood function for all observations $[(t,j)_1, \cdots, (t,j)_N]$ is given by:

$$\text{L}(\theta) = \prod_{n=1}^{N} \text{Prob}((t,j)_n|\theta) \tag{4}$$

This enables the estimation of the parameters θ by maximizing the likelihood function numerically using the R package maxLik by Henningsen and Toomet (2011). Of all tested distribution families for the residence times $p_i(\cdot;\theta)$, the Gamma distributions were selected as they led to the highest log likelihood (Gamma: −511.4, Lognormal: −514.7, Weibull: −513.1).

As no observation of the time at which the diet left PMG2 was available, the residence time in this region was estimated by scaling the residence time of PMG1 based on the mean region lengths:

$$X_4 = \frac{l_{PMG2}}{l_{PMG1}} X_3 \quad (5)$$

where the mean length of PMG2 (1.6 cm) is denoted by l_{PMG2} and the mean length of PMG1 by l_{PMG1} (2.8 cm).

2.1.7. Determination of diet intake

Diet intake is the amount of diet ingested by the larvae at different time points and can be estimated by measuring the absorbance of the dye in BSFL gut samples at 628 nm (Kim et al., 2018; Rodrigues et al., 2015). At the time points 20, 90, and 180 min, for each artificial diet and experiment, five midguts from randomly selected larvae were placed in separate 1.5 mL tubes containing 300 μL phosphate buffered saline and two metal beads (diameter: 3 mm; Uiker AG, Switzerland). Tissues were homogenized by mixing the tubes on a vortex for 30 s. Following homogenization, tubes were centrifuged at 20,000 × g for 10 min at 4 °C, and the supernatant was stored at −20 °C until spectrometric analysis.

Following thawing, the absorbance was measured in triplicate with 300 μL of each gut homogenate at 628 nm and 750 nm using a spectrometer (Genesys 10S, Thermo Fisher, Scientific, Waltham MA, USA). The mean absorbance at 750 nm was subtracted from the mean absorbance at 628 nm to eliminate the absorbance offset induced by other constituents in the sample (Wetzel and Likens, 2000). This net absorbance was converted into mg of wet and dry diet intake using a calibration curve. The calibration curve was produced by linear regression from absorbance values measured in triplicate for the three artificial diets containing the same amount of water as in the feeding experiments and 0.0001, 0.0002, 0.0004, and 0.0008% (w/v) Blue 1 (see Fig. S2). The protein and NFC intake were calculated by multiplying the diet intake with the protein and NFC content of the respective artificial diet (Table 1) and the caloric intake was estimated according to Gold et al. (2020). It should be noted that determining diet and nutrient intake with this approach assumed that the entire diet was ingested by BSFL.

2.1.8. Statistical analysis

Analysis of variance (ANOVA) followed by pairwise Tukey post-hoc comparisons were conducted to test i) the effect of the experimental repetition on the larval morphometric parameters (i.e., cephalic capsule width, wet larval weight, length of midgut regions, and total midgut length), ii) the effect of the artificial diet nutrient composition on diet, energy, protein, and NFC intake. The homogeneity of variance and normality between the different groups of comparison were assessed graphically (see Fig. S3 to S5). A p-value < 0.05 was chosen to denote significance. Two data points, identified as outliers, were removed from the diet intake data before statistical analyses using the Median Absolute Deviation (MAD) method and a threshold of three MADs (Leys et al., 2013). The analysis was conducted using R version 3.6.2 (R Core Team, 2017).

2.2. In vitro digestions

2.2.1. Diets

In vitro digestions were performed using the same artificial diets used for determination of diet midgut residence times. To validate the midgut simulations with different diet contents, additionally, an artificial diet with 7:78:11% DM protein:NFC:fibre, referred to as P^7NFC^{78}, and five biowastes previously used in *in vivo* feeding experiments were used (Gold et al., 2020) (Table 1, Table S1).

2.2.2. Digestion protocol

The *in vitro* simulations of BSFL midgut digestion were based on the INFOGEST 2.0 method developed to mimic human gastrointestinal food digestion (Brodkorb et al., 2019). This method was adapted considering the available information for BSFL digestion (i.e., pH and enzymes: Bonelli et al. (2019), temperature: Bloukounon-Goubalan et al. (2019), Table 2) and the diet residence times estimates. In addition, bile salts and pepsin were not considered as they are not present in insects or not yet studied in BSFL (Behmer and Nes, 2003). Gastric lipase was also not considered despite its presence in the BSFL AMG and PMG (Bonelli et al., 2019). Simulated digestion fluid amounts were changed as no information is available on the digestion fluids of BSFL, and use of the same fluid volume as in the human digestion model would increase the costs of enzymes and compromise the determination of supernatant nutrients. In comparison to the doubling of the simulated digestion fluids with each gut region starting from a ratio of 1:1 (w diet/w fluid) in the INFOGEST 2.0 method, 1 mL of simulated digestion fluid was added in this research per midgut region.

The *in vitro* digestions were carried out with chemicals of analytical grade in duplicate on artificial diets and in triplicate on biowastes with the conditions summarized in Table 2. For each digestion, approximately 1 g of diet was placed into a 50 mL falcon tube and digested in a water bath (Corio C, Julabo AG, Germany) at 37 °C, within the range of typical substrate temperatures in BSFL treatment (33–45 °C, Bloukounon-Goubalan et al. (2019)). The artificial diets were mixed with deionized water to 80% moisture content, and biowastes were used as received (see Gold et al., 2020 for details). The pHs in the three midgut regions were adjusted with 2 M HCl and 0.1–6 M NaOH (Slimtrode, Metrohm AG, Switzerland). The enzymes used were α-amylase from human saliva (EC 3.2.1.1), trypsin from porcine pancreas (EC 3.4.21.4), and α-chymotrypsin from bovine pancreas (EC 3.4.21.1) (Brodkorb et al., 2019). Further details regarding enzyme activity and the *in vitro* digestion protocol are included in the Supplementary Material.

Following digestion in the PMG, 6 M HCl was added to stop enzyme activity. The digestion fluids were centrifuged at 14,000 × g for 45 min at 4 °C. The supernatants were immediately frozen with liquid nitrogen and stored at −20 °C until further analyses. The pellets were dried in a laboratory oven at 80 °C for 24 h.

2.2.3. Digestion products

A typical approach for evaluating *in vitro* digestion model outcomes is determination of nutrients in digestion products (Kiers et al., 2000; McClements et al., 2009; Oomen et al., 2002, 2003). We determined diet digestibility, and supernatant maltose, glucose, total organic carbon (TOC), total nitrogen (TN) and amino acids. These parameters were selected as estimates of NFC (i.e., maltose and glucose), protein (i.e., total nitrogen and amino acids) and organic matter (i.e., total organic carbon). NFC, protein and organic matter have previously been shown to be important for BSFL development (Barragán-Fonseca et al. 2018b, Barragán-Fonseca et al. 2018a; Beniers and Graham 2019; Gold et al., 2020; Lalander et al. 2019).

Maltose and glucose were determined as D-glucose using a commercial enzymatic kit (Megazyme, Total Starch Assay K-TSTA). The supernatant was mixed with 4.5 mL of 100 mM sodium acetate buffer (pH 4.5) and 0.1 mL amyloglucosidase (3,300 U/mL) and incubated at 50 °C for 30 min. D-glucose was quantified at 510 nm against a standard, following incubation with 3.0 mL GOPOD reagent at 50 °C for 20 min. The TN and TOC were determined with the 680 °C combustion catalytic oxidation method according to the manufacturer's instructions (TOC-L Analyzer, Shimadzu Corporation, Japan). Amino acids (except for tryptophan) were analyzed in the pool of the supernatants from the *in vitro* digestion replicates for each biowaste with a Waters AccQ-Tag Ultra Derivatization Kit and Waters UPLC system with an Acquity UPLC Binary Solvent Manager and Sample Manager, based on the manufacturer instructions and previous research (see detailed pro-

Table 2
In vitro digestion conditions used in this study.

	Digestion fluid[1]		Enzyme concentration[2]	pH[2]	$CaCl_2$[1]	MiliQ water	Residence time[3]
	Type	Volume					
-	–	mL	U/mL[2]	–	µL (0.3 M)	mL	min
AMG	Salivary	0.8	6.4 (amylase)	6	5	Top up to total fluid volume	15
MMG	Gastric	0.8	–	2	0.8	addition of 1 mL per midgut region	45
PMG	Intestinal	0.35	4 (amylase), 9.5 (trypsin), 53 (chymotrypsin)	8.5	4		90

[1] Brodkorb et al. (2019).
[2] Bonelli et al. (2019).
[3] Results of this study (see Section 3.1, Table 4).

tocol in the Supplementary Material). The TN and TOC results of *in vitro* digestion samples without diet were used to correct TN and TOC results for nitrogen and organic carbon included in the digestion fluids and enzymes. Maltose and glucose, TOC, and TN concentrations were normalized (g/L × g DM) based on the amount of diet digested using equation (6):

$$\text{Supernatant sugar, TN, TOC} = \frac{supernatant\ sugar, TN, TOC\ \left(\frac{g}{L}\right)}{diet\ input_{dry\ mass}\ (g\ DM)} \quad (6)$$

The diet digestibility (as % DM) was calculated analogous to *in vivo* waste reduction (Gold et al., 2020) using equation (7) based on the dry mass of the pellet following centrifugation:

$$\text{Diet digestibility} = \left(1 - \frac{pellet_{dry\ mass}\ (g\ DM)}{diet\ input_{dry\ mass}\ (g\ DM)}\right) \times 100 \quad (7)$$

2.3. In vivo feeding experiments

In vivo feeding experiments were executed with the same artificial diets and biowastes used in *in vitro* digestions. Waste reduction and larval weight was calculated as described in Gold et al. (2020). For each artificial diet, 2–3 replicates with 40 BSFL with an initial weight of 5.4 mg DM were placed in plastic containers (5.5 cm diameter, 7.2 cm height) and fed every three days at a feeding rate of 30 mg DM/(larva × day) for a total of six days. Experiments were replicated three times. Feeding experiment results with biowastes were taken from Gold et al. (2020). For each biowaste, 4–5 replicates with 80 BSFL with an initial weight of 3.8 mg DM were placed in plastic containers (7.5 cm diameter, 11 cm height) and fed every three days at a feeding rate of 27 mg DM/(larva × day) for a total of nine days. Experiments were conducted once. All experiments were conducted without light in a climate chamber (HPP 266, Memmert GmbH, Germany, 28 °C, 70% relative humidity).

2.4. Comparison of in vivo and in vitro results

Results from *in vitro* digestions and *in vivo* feeding experiments were compared to assess whether the *in vitro* model can be indicative of feeding experiment results. Since *in vivo* feeding experiment designs typically vary between studies (Bosch et al., 2020) and static *in vitro* models are oversimplified (Bohn et al., 2018), we regarded a ranking method to be more meaningful than comparison of absolute results. For example, absolute diet digestibility can be expected to be much lower than waste reduction considering it is calculated following one digestion, whereas waste reduction is calculated following several digestions.

Ordinal ranking (e.g., 1, 2, 3) was applied separately to artificial diets and biowastes as per the mean results of the *in vitro* digestion products and *in vivo* performance metrics, considering the range of results for each parameter. Fractional ranking (e.g., 1, 2–3, 4) was applied when the mean value (±standard deviation for n > 2, ± differences between repetition for n = 2) overlapped among diets. Lower ranks were given to diets with higher *in vitro* digestion products and higher *in vivo* performance metrics.

The ranking of diets based on *in vitro* diet digestibility was compared to *in vivo* waste reduction. A mean rank of the three *in vitro* supernatant nutrient parameters was calculated and compared to *in vivo* larval weight. The *in vitro* model was deemed indicative of *in vivo* feeding experiments results if diets received the same rank. Comparison between *in vitro* digestion products and *in vivo* feeding experiment metrics is justified considering that diet digestibility and waste reduction are calculated in a similar way (Gold et al., 2020, Equation (7)), and that previous studies concluded that diet NFC, protein and organic matter can increase larval weight (Barragán-Fonseca et al. 2018b, Barragán-Fonseca et al. 2018a; Beniers and Graham 2019; Gold et al., 2020; Lalander et al. 2019).

3. Results and discussion

3.1. Diet midgut residence times

The present study determined, for the first time, diet midgut residence times and diet intake using artificial diets varying in protein and NFC content. Cephalic capsule width measurements identified BSFL used for residence time determination as late fifth instar/beginning sixth instar in all experiments (Table 3). Despite significant differences in wet larval weight between experiments, the length of the different midgut regions and total midgut length was not significantly different between experiments (Table 3). Therefore, to increase the quality of the residence time estimations, results of the foremost position of the dye in the midgut for the three experiments were pooled for modeling the midgut residence time distributions.

The probability density functions of the foremost colored artificial diet position over time in the three midgut regions are shown in Fig. 1. The shape of the distributions demonstrates considerable variability in residence times between larvae grown on the same diet. This has also been previously reported for drone fly larvae (*Eristalis tenax*) (Waterhouse, 1954) and could be attributed to differences between larvae during development (e.g., due to differences in nutrient provision in previous life stages), physiological condition (e.g., molting), and the corresponding individual nutritional demand (Chapman, 2013; Edgecomb et al., 1994), or length of midgut regions and total midgut length (see standard deviation of midgut region lengths between larvae in Table 3).

As static *in vitro* models do not consider residence time distributions, descriptive statistics (i.e., mean, median, mode) of the probability density functions were calculated and are included in Table S2. In order to neither under- nor overestimate the diet res-

Table 3
Mean morphometric parameters of BSFL used for determining diet midgut residence times.

	Unit	n*	Experiment 1	Experiment 2	Experiment 3
Cephalic capsule width	mm	10	1.03 (0.08)	1.00 (0.06)	1.05 (0.07)
Larval weight	mg	75	219 (28)	177 (36)	186 (31)
AMG length	cm	10	2.5 (0.2)	2.5 (0.2)	2.5 (0.2)
MMG length	cm	10	1.5 (0.2)	1.5 (0.2)	1.7 (0.2)
PMG length	cm	10	4.2 (0.8)	4.2 (0.4)	4.6 (0.5)
Midgut length	cm	10	8.2 (1.1)	8.2 (0.6)	8.8 (0.7)

In parenthesis: standard deviation; AMG: Anterior midgut; MMG: Middle midgut; PMG: Posterior midgut.
* n = number of larvae used per morphometric parameter.

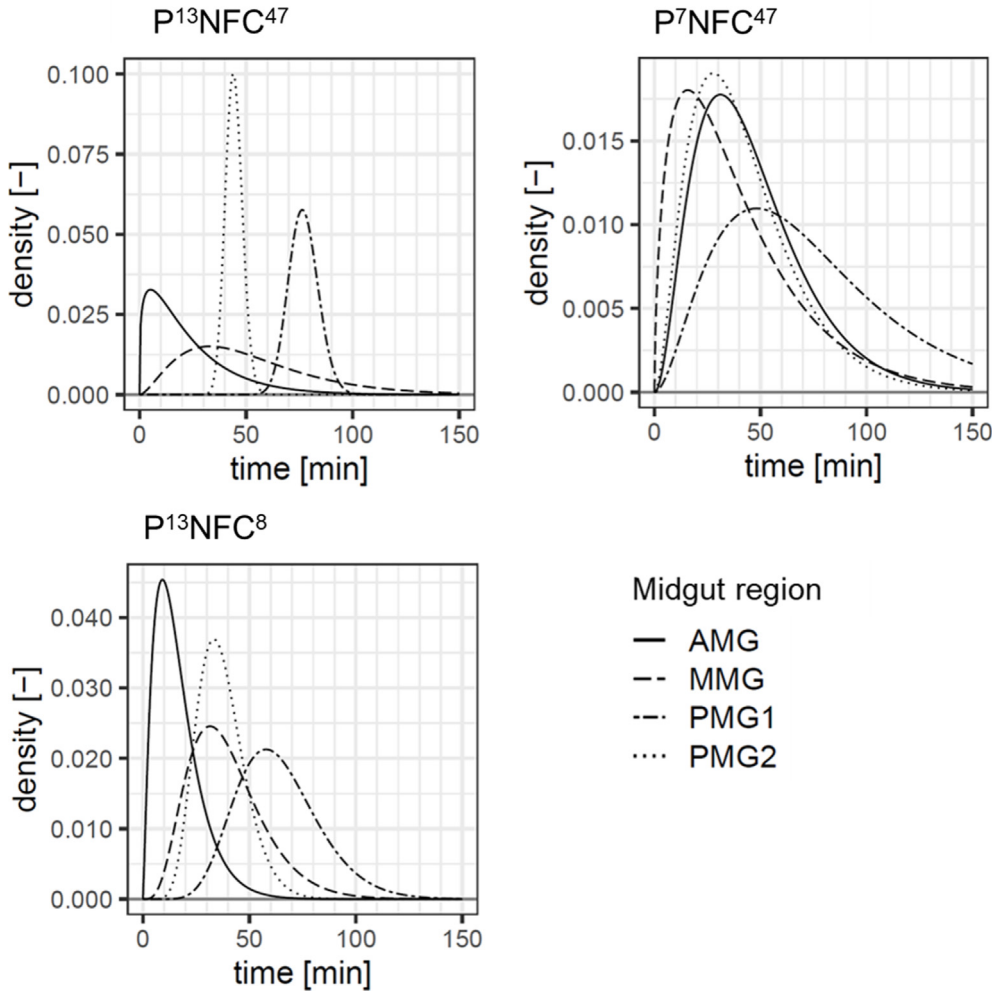

Fig. 1. Probability density functions of the BSFL midgut residence time for the three artificial diets. AMG: Anterior midgut, MMG: Middle midgut, PMG: Posterior midgut. See Table 4 for the medians of probability density functions.

idence time when modelling the BSFL midgut, the median (Table 4), which is more robust to outliers than the mean, was selected as the most meaningful parameter. In the following text, the median residence time is presented together with the mean ± standard devi-

Table 4
Median of probability density functions of the BSFL midgut residence time distributions (min) with three artificial diets varying in protein and NFC content. See Fig. 1 for probability density functions and Table S2 for more descriptive statistics.

Diets	n*	AMG	MMG	PMG 1	PMG 2	Total
$P^{13}NFC^{8}$	233	14	37	62	36	154
$P^{13}NFC^{47}$	218	17	46	77	44	191
$P^{7}NFC^{47}$	176	41	32	65	37	195

AMG: Anterior midgut; MMG: Middle midgut; PMG: Posterior midgut; n: number of larvae.
* n = total number of larvae dissected per diet..

ation in parenthesis. As the distributions do not always follow a bell-shaped curve, residence time estimates depended on the descriptive statistic used. However, the overall trends in diet residence times between midgut regions and artificial diets presented in the following section also hold true for the other descriptive statistics. The diet residence time estimates are considered to be more reliable for AMG to PMG1 as they were based on the foremost dye position, whereas the PMG2 residence time was interpolated based on midgut length. Therefore, in the following presentation of PMG diet residence time results, PMG1 and PMG2 are given separately; the residence time estimate for PMG2 is supported by the collected experimental data.

Despite the variability between larvae, the results of this study demonstrate that diet residence time in the different midgut regions of BSFL is influenced by the protein and NFC content in the diet. As the NFC content correlates negatively with the cellulose and caloric content in the diet (Table 1), these parameters are also likely decisive for the diet residence time in BSFL. In addition, the diet intake in BSFL was measured to propose explanations for the observed residence times between diets. Diet intake and midgut residence time are likely connected; the more diet is ingested, the faster the gut content is pushed forward, reducing the diet midgut residence time (Karasov et al., 2011).

For the three artificial diets, the overall midgut residence time was 154 min (156 ± 31 min) for $P^{13}NFC^{8}$, 191 min (197 ± 38 min) for $P^{13}NFC^{47}$, and 195 min (202 ± 64 min) for $P^{7}NFC^{47}$. These results indicate that residence times in the BSFL midgut were shorter than those in the guts of other dipteran larvae, although this difference could also be due to different diets across studies. In fruit fly larvae (*Drosophila melanogaster*), which are much smaller, the diet takes approximately 30 min to reach the PMG. Mumcuoglu et al. (2001) and Waterhouse (1954) reported total gut residence times of 60–90 min for green bottle fly larvae (*Lucilia sericata)* and 85–120 min for drone fly larvae. Considering the midgut length, this corresponds to a passage rate of 50–75 mm/h for drone fly larvae in comparison to 29–36 mm/h for BSFL (AMG to PMG2).

Except for the diet lower in protein content, the residence time was shortest in the AMG and the longest in the PMG (Table 4, Fig. 1). Diets also had the longest residence time in the PMG of housefly larvae (*Musca domestica*) (Espinoza-Fuentes and Terra, 1987) and different species of blow fly larvae (Waterhouse, 1954). The high digestive capability (i.e., high enzymatic activity and diet residence time) and the morphological features of the fly larvae PMG suggests that this midgut region plays a fundamental role in the decomposition of nutrients to monomers and in their absorption (Bonelli et al., 2019; Gold et al. 2018a). In addition, as the growth of bacteria is time-dependent, the higher diet residence time may be a contributor to the bacterial count in the PMG, which is higher than that in the AMG and MMG (Bruno et al., 2019).

Diet AMG residence times decreased with the diet protein content. As illustrated in Fig. 1, $P^{7}NFC^{47}$ had an AMG residence time of 41 min (46 ± 26 min) in comparison to 14 (16 ± 11 min) and 17 min (23 ± 2 0 min) for $P^{13}NFC^{8}$ and $P^{13}NFC^{47}$, respectively. As BSFL are unable to select their nutritional environment, the increase in the AMG residence time could be a post-ingestive mechanism to balance nutrient intake. Following ingestion, insects and their associated microbiota may balance nutrient decomposition and absorption. For example, locusts (*Locusta migratoria*) regulate macronutrient digestion and absorption, among others, through the amount of enzymes secreted into the gut, secreting fewer enzymes for nutrients in excess and more enzymes for nutrients in deficit (Clissold et al. 2010; Zanotto et al., 1993). Similar mechanisms were found in the common fruit fly by Miguel-Aliaga et al. (2018). In BSFL, Bonelli (Marco Bonelli, personal communication, University of Milan, 2020) observed protease activity in the AMG for low-protein diets while proteases were almost absent in this region in larvae reared on diets with excess protein. In addition to adjusting enzyme activities, prolonging the AMG diet residence time could be an additional post-ingestive mechanism of BSFL to improve protein digestion. As shown in Fig. 2, protein ingestion was lowest for $P^{7}NFC^{47}$. Thus, as nutrient extraction efficiency is positively correlated with diet residence time (Karasov et al., 2011), BSFL could have increased access to free amino acids (which are indispensable for fly larval development) by increasing AMG diet residence time (Colombani et al., 2003; Danielsen et al., 2013; de Carvalho and Mirth, 2017; Lalander et al., 2019). This hypothesis could be tested in future research by measuring both midgut lumen enzyme activities and residence times between diets varying in protein content.

Diet NFC, and thereby cellulose and energy content, also appeared to have a significant influence on both diet ingestion and overall midgut residence time. For the diets higher in protein ($P^{13}NFC^{8}$ and $P^{13}NFC^{47}$), MMG and PMG diet residence times increased with the diet NFC content and decreased with the diet cellulose content. MMG and PMG residence times were 46 and 77 min for $P^{13}NFC^{47}$ in comparison to 37 and 62 min for $P^{13}NFC^{8}$, respectively. As shown in Fig. 2, this decrease in MMG and PMG residence time meant that larvae ingested significantly more of the $P^{13}NFC^{8}$ diet than the other two diets. Lowering of the diet midgut residence time could be an indication of compensatory feeding in BSFL due to nutrient restrictions (i.e. low digestible nutrient and caloric content). Compensatory feeding has been reported for several other Dipteran species (Carvalho et al., 2005; Gelperin and Dethier, 1967; Simpson et al., 1989) and indicates that BSFL increase their diet intake and thereby lower the diet residence time to compensate for the low caloric content of $P^{13}NFC^{8}$. However, as shown in Fig. 2, despite the increased diet ingestion, larvae ingested significantly less digestible energy by feeding on $P^{13}NFC^{8}$ than of the other two diets that are higher in NFC.

In summary, our results demonstrate that total and midgut region residence time in BSFL is influenced by the diet nutrient content. This influence is often neglected in *in vitro* models of humans and farmed animals. Depending on the diet nutrient content, *in vitro* models may over- or under-estimate *in vivo* performance based on the soluble nutrients in the supernatant. For example, as enzyme activity is the amount of substrate (e.g., starch) catalyzed per minute, the supernatant nutrient content as measured in this study (see Section 3.2) is proportional to the residence time when substrates are available in excess and no inhibitors are present. However, not mimicking the influence of diet nutrients, and other parameters such as sex, instar, body size, and age, which have all been shown to influence diet residence time, is also one of the strengths of the model as it allows for cost-effective implementation. Diet residence times of 15 min in the AMG, 45 min in the MMG, and 90 min in the PMG were used in subsequent *in vitro* simulations of the BSFL midgut.

3.2. In vitro simulation of midgut digestion

The residence time estimates were used to mimic the BSFL midgut *in vitro* for the first time. As validation of the *in vitro* digestion model, the study assessed whether ranking of the diets based on *in vitro* digestion products is similar to the ranking of diets based on waste reduction and larval weight recorded in *in vivo* feeding experiments.

Based on the *in vitro* simulations, $P^{7}NFC^{78}$ and $P^{13}NFC^{47}$, and canteen and slaughterhouse wastes were expected to have the highest waste reduction and larval weight in *in vivo* feeding experiments. Diet digestibility (Table 5) and supernatant nutrient content (Table 6) were highest for these diets, likely due to their highly digestible nutrient content (i.e., protein, NFC, and lipids,

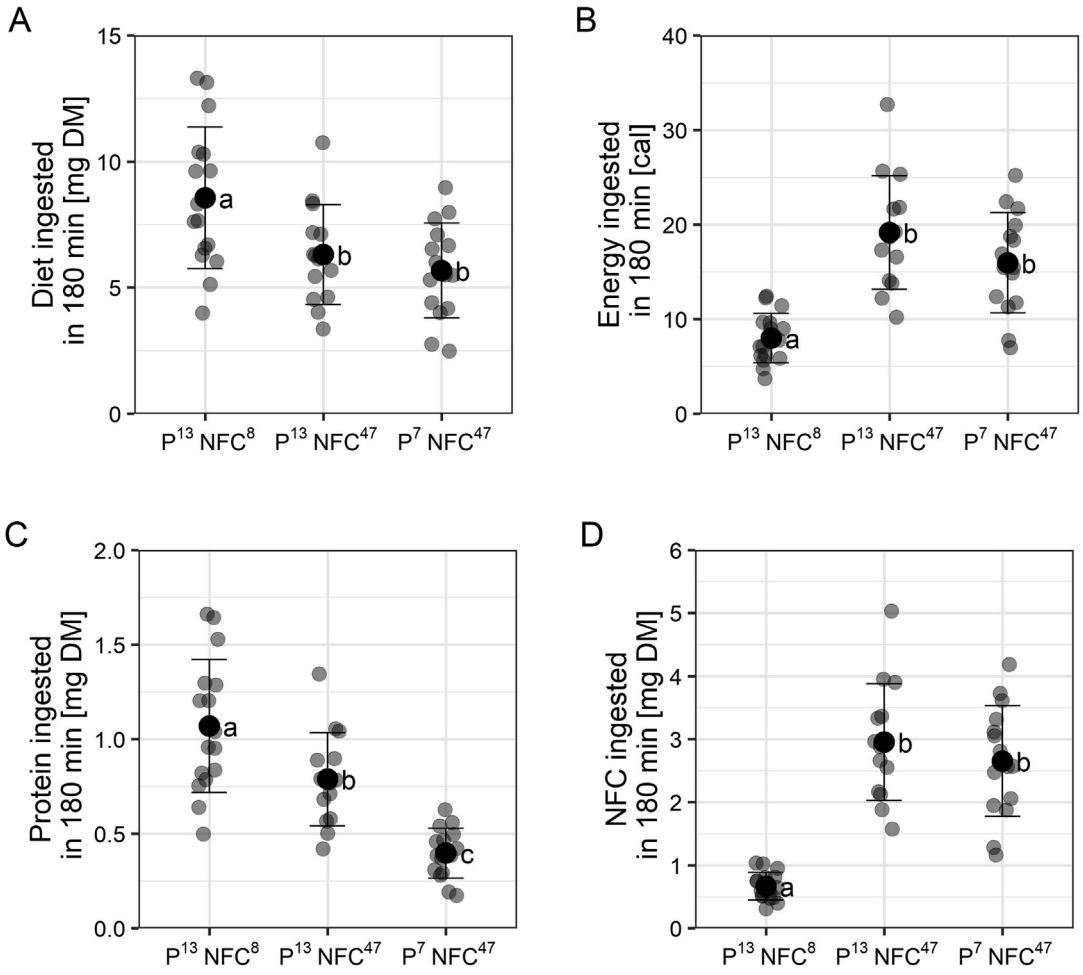

Fig. 2. Mean diet (mg DM) (A), energy (cal) (B), protein (mg DM) (C), and NFC (mg DM) (D) ingested by BSFL in 180 min on the three artificial diets. Means, standard deviations, and results per larvae are displayed for all three experiments. Results with no shared letter are significantly different from each other.

Table 5
Mean digestibility of diets in *in vitro* simulations of the BSFL midgut and waste reduction in *in vivo* feeding experiments. The asterisks indicate diets for which the ranking based on *in vitro* results deviated from the ranking of the diets based on *in vivo* feeding experiments.

	in vitro Diet digestibility		*in vivo* Waste reduction	
	% DM	Rank	% DM	Rank
Artificial diets				
$P^{13}NFC^{8}$	15.0 (4.6)	4	31.7 (1.8)	4
$P^{13}NFC^{47}$	30.0 (2.8)	2	48.9 (3.9)	1–2
$P^{7}NFC^{78}$*	37.2 (2.5)	1	41.0 (1.4)	3
$P^{7}NFC^{47}$*	26.5	3	47.0 (3.4)	1–2
Biowastes				
Cow manure	11.4 (10.6)	4–5	12.7 (0.9)	5
Mill by-products*	19.0 (3.6)	4–5	56.4 (1.2)	1–2
Canteen waste	45.0 (14.6)	1–3	37.9 (3.8)	3
Poultry slaughterhouse waste*	36.9 (1.4)	1–3	30.7 (4.7)	4
Vegetable canteen waste	49.9 (5.6)	1–3	58.4 (1.4)	1–2

In parenthesis: standard deviation for samples where n ≥ 3 and differences between analyses where n = 2.
In vivo results for biowastes were taken from Gold et al. (2020).

see Table 1). Accordingly, $P^{7}NFC^{47}$ and $P^{13}NFC^{8}$, which are lower in protein and/or NFC, and cow manure and mill by-products, which are richer in fiber and/or have lower organic matter content, received a higher ranking, indicating that a lower *in vivo* waste reduction and larval weight can be expected. The correlation between *in vitro* digestion product results and the diet nutrient composition indicates that the *in vitro* model could also complement and/or replace conventional diet gross nutrient composition analyses (see parameters in Table 1) frequently completed for BSFL diets.

Comparison of the ranking based on *in vitro* results and the ranking based on the *in vivo* performance shows that *in vitro* simulations can predict *in vivo* outcomes. The approach was able to broadly distinguish between the best and the worst performing

Table 6
Mean supernatant nutrient content following *in vitro* simulation of the BSFL midgut and larval weight and bioconversion rate results of *in vivo* feeding experiments. The asterisks indicate diets for which the ranking based on *in vitro* results deviated from the ranking of the diets based on *in vivo* feeding experiments.

	in vitro Glucose & Maltose		Total nitrogen		Amino acids		Total organic carbon		Supernatant nutrients	*in vivo* Larval weight	
	g/(L × g DM)	Rank	g/(L × g DM)	Rank	g/L	Rank	g/(L × g DM)	Rank	Mean Rank	mg DM	Rank
Artificial diets											
$P^{13}NFC^{8}$	0.6 (0.1)	4	3.3 (0.7)	1–2	–	–	17.5 (2.6)	4	3/3–4	21.0 (2.1)	4
$P^{13}NFC^{47}$	3.8 (0.6)	2–3	3.7 (0.6)	1–2	–	–	30.9 (3.6)	1–2	2/1–2	47.5 (2.5)	1
$P^{7}NFC^{78}$*	6.8 (0.2)	1	2.7 (0.2)	3	–	–	38.6 (1.8)	1–2	2/1–2	32.7 (2.2)	3
$P^{7}NFC^{47}$*	3.6 (0.5)	2–3	1.8 (0.3)	4	–	–	23.8 (0.9)	3	3/3–4	41.5 (0.2)	2
Biowastes											
Cow manure	0 (0)	4–5	1.7 (0.3)	–	0.5 (0.1)	5	10.7 (1.0)	5	5/5	14.3 (0.4)	5
Mill by-products	1.7 (0.3)	2–3	3.5 (0.1)	–	1.8 (0.1)	3–4	24.6 (0.5)	4	3/3–4	41.7 (0.9)	3
Canteen waste	1.5 (0.3)	2–3	9.1 (2.2)	–	5.5 (0.7)	2	47.7 (7.2)	1–3	2/1–2	44.2 (5.9	2
Poultry slaughterhouse waste	0 (0)	4–5	12.4 (0.7)	–	9.9 (2.8)	1	44.4 (2.4)	1–3	3/3–4	39.4 (0.7)	4
Vegetable canteen waste	3.6 (0.3)	1	3.3 (0.1)	–	1.9 (0.3)	3–4	49.3 (0.3)	1–3	2/1–2	59.1 (2.6)	1

In parenthesis: standard deviation for samples where n ≥ 3 and differences between analyses where n = 2.
In vivo results for biowastes were taken from Gold et al. (2020)
See Section 2.4 for the applied ranking procedure.

diets (Tables 5 and 6). For example, $P^{13}NFC^{8}$ and $P^{7}NFC^{47}$, and vegetable canteen waste and cow manure received the same ranking based on *in vitro* simulations and *in vivo* feeding experiments. This confirms that the ranking of biowastes based on results of digestion products from *in vitro* digestion could be a valuable tool for screening of different biowastes based on BSFL treatment performance.

3.3. Simulation limitations

Despite these promising results, several differences between the *in vitro* and *in vivo* ranking (Tables 5 and 6) highlighted the limitations of the laboratory-based simulation, digestion product analyses, and/or the applied ranking procedure. In particular, the ranking based on *in vitro* digestion products was i) unable to predict the differences in *in vivo* performance between vegetable canteen waste, canteen waste, and poultry slaughterhouse waste; ii) overestimated the *in vivo* performance of $P^{7}NFC^{78}$ and poultry slaughterhouse waste; and iii) under-estimated the *in vivo* performance of mill by–products.

These discrepancies are to be expected as static *in vitro* digestion models are oversimplified and do not include all complex and dynamic digestion processes (Bohn et al., 2018). For example, dynamic changes in temperature during BSFL treatment (Bloukounon-Goubalan et al., 2019), multiple digestions of the diet by BSFL, differences in properties of enzymes in the midgut lumen and commercial enzymes, dynamic changes in enzyme activities in relation to the nutritional environment (Benkel and Hickey, 1986; Clissold et al., 2010), external digestion (Sakaguchi and Suzuki, 2013), and lipases, lysozymes, and chitinases (Bonelli et al., 2019; Terra and Ferreira, 2012) in the fly larvae midgut were not considered in this study. An additional explanation for the mismatch between the *in vitro* and *in vivo* ranking could be false assumptions regarding the effect of supernatant nutrients on larval weight. The current study did not estimate nutrient bioavailability and/or bioactivity to BSFL (McClements et al., 2009), but instead assumed that all nutrients released from the diet during *in vitro* simulation are absorbed by the larvae into the hemolymph, metabolized, and contribute to larval growth (Oomen et al., 2002, 2003). In addition, the procedure of this study assumed that all nutrients measured in the supernatant have the same linear effect on larval weight. This might be an oversimplification as previous work on BSFL and common fruit fly larvae indicate that protein can be more important than NFC in determining larval weight and development time (Danielsen et al., 2013; de Carvalho and Mirth, 2017; Lalander et al., 2019). In addition, insufficiency or excess of nutrients or poor nutrient ratios (e.g., protein to NFC) affect larval development (Barragán-Fonseca et al. 2018b; Gold et al., 2020).

The lack of detailed knowledge on BSFL biology currently limits mimicking all these processes in an *in vitro* model. This would also be impractical considering the costs involved (e.g., enzyme costs). However, based on this validation of the simulated midgut, future studies should assess whether a stronger correlation can be established between *in vitro* and *in vivo* results by considering the nutrient requirements of BSFL. Fly larvae adjust their diet intake and digestion based on their nutritional environment and nutritional needs (see Section 3.1). For example, fly larvae control diet intake based on protein, and over- or under-consuming other nutrients such as sugars (de Carvalho and Mirth, 2017). In addition, digestion of excess nutrients, such as sugars, can result in metabolic costs, decreasing larval weight and increasing development time (Matzkin et al., 2011; Musselman et al., 2011). This mechanism could explain the overestimation of the *in vivo* performance based on *in vitro* results for $P^{7}NFC^{78}$ and slaughterhouse waste. These diets are unbalanced in terms of nutrient content and nutrient ratios (Table 1), compared to nutritionally balanced diets for BSFL (e.g., protein to NFC ratios of 2:1 – 1:4, NFC content < 40%) (Barragán-Fonseca et al. 2018b; Gold et al., 2020). $P^{7}NFC^{78}$ was high in NFC, while the slaughterhouse waste was high in protein. An additional explanation for their lower performance *in vivo* than *in vitro* could be suboptimal diet palatability (Cohen, 2005). In contrast to all other diets, the slaughterhouse and canteen wastes were more digestible *in vitro* than *in vivo*, supporting the hypothesis that BSFL do not digest all of these nutrients *in vivo*, owing to adjustments in diet intake and digestion that are, in turn, governed by poor nutrient contents and/or ratios or suboptimal diet palatability.

Further research could also consider simulating the midgut microbiota. In BSFL treatment, microbes in the biowaste and/or midgut are able to use diet constituents as nutrient sources and thereby likely contribute to waste reduction. Microbes produce digestible biomass and metabolites (e.g., short chain fatty acids) for BSFL that can contribute to larval growth (Douglas, 2010, 2009; Lam et al., 2009; Romero et al., 2006; Wong et al., 2014). Microbial-mediated processes can be especially valuable on nutrient poor diets and/or on diets that are constituted by nutrients that are indigestible by BSFL, such as hemicelluloses (Storelli et al., 2011; Zhao et al., 2017). Similar to intestinal digestion in humans, microbial enzymes (e.g., β-glucanases, xylanases, and pectinases) (Terra and Ferreira, 2012) in the biowaste and/or the midgut may bring about partial digestion of hemicelluloses in BSFL treatment (Bruno et al., 2019; De Smet et al., 2018; Gold et al., 2020,

2018a; Jeon et al., 2011; Lee et al., 2014; Rehman et al., 2017). This was not considered in this study and could explain why mill by-products, which are mainly plant cell walls consisting of hemicelluloses (such as xylans or β–glucans) (Merali et al., 2015), had a lower performance in the *in vitro* simulation than in *in vivo* feeding experiments (Tables 5 and 6). As an initial step of microbial simulation in the BSFL midgut, PMG could serve as the primary area of focus, owing to the longest diet residence time (Section 3.1) and the highest bacterial load (Bruno et al., 2019) in this region. Microbial fermentation could be considered by the addition of enzymes, specific microbes isolated from the PMG, or the entire PMG content (Wahlgren et al., 2019).

4. Conclusions

The present study is the first to evaluate *in vitro* simulation of the BSFL midgut. Despite not completely mimicking the complexity of the BSFL digestive system, such as differences in midgut residence times with diet nutrient content, *in vitro* simulations were able to predict the outcomes of *in vivo* feeding experiments. Digesting diets in an *in vitro* model and subsequent analyses of the formed digestion products indicated *in vivo* BSFL waste reduction and larval weight, and diet nutrient composition. For several diets, the performance estimated based on *in vitro* results did not match with the results in the feeding experiments. More reliable estimates of *in vivo* feeding experiment outcomes could presumably be provided by considering the nutrient requirements of BSFL, hemicellulose digestion, and the diet and gut microbiota. However, the main advantages of *in vitro* simulations are their simplicity and low cost. Thus, the benefits of simulations resulting in more accurate mimicking of digestive processes needs to be balanced with the added resources required for their implementation (e.g., laboratory equipment, consumables, labor).

Authorship contribution statement

Moritz Gold: Conceptualization, Methodology, Investigation, Formal analysis, Visualization, Writing - original draft, Funding acquisition. **Julia Egger:** Conceptualization, Methodology, Investigation, Formal analysis, Visualization, Writing - review & editing. **Andreas Scheidegger:** Methodology, Formal analysis, Visualization, Writing - review & editing. **Christian Zurbrügg:** Conceptualization, Supervision, Project administration, Funding acquisition. **Daniele Bruno:** Methodology. **Marco Bonelli:** Methodology. **Gianluca Tettamanti:** Methodology, Writing - review & editing. **Morena Casartelli:** Methodology, Writing - review & editing. **Eric Schmitt:** Conceptualization, Methodology, Writing - review & editing. **Ben Kerkaert:** Investigation, Formal analysis. **Jeroen De Smet:** Supervision, Methodology, Writing - review & editing. **Leen Van Campenhout:** Supervision, Writing - review & editing. **Alexander Mathys:** Conceptualization, Supervision, Project administration, Writing - review & editing, Funding acquisition.

Declaration of Competing Interest

The authors declared that there is no conflict of interest.

Acknowledgements

This research was funded by the Sawiris Foundation for Social Development (Engineering for Development (E4D) Scholarship Program), Eawag, the ETH Zurich Foundation, ETH Global, and Bühler AG. Jeroen de Smet holds a postdoctoral fellowship grant (grant number: 12V5219N) of the Research Foundation – Flanders. The authors are grateful to Jonathan Cammack and Jeffery K. Tomberlin from Texas A & M University regarding the production of the artificial insect diets, and to Christian Nansen, Trevor Fowles, Moriah Garrison and Miles Dakin from UC Davis for their comments on an earlier version of the manuscript. Also, the authors thank the Functional Genomics Center Zurich for providing amino acid analyses, especially Dr. Birgit Roth Zgraggen and Dr. Chia-wei Lin.

Appendix A. Supplementary material

Supplementary data to this article can be found online at https://doi.org/10.1016/j.wasman.2020.05.026.

References

Barragán-Fonseca, K.B., Dicke, M., van Loon, J.J.A., 2018a. Influence of larval density and dietary nutrient concentration on performance, body protein, and fat contents of black soldier fly larvae (*Hermetia illucens*). Entomol. Exp. Appl. 166, 761–770.

Barragán-Fonseca, K.B., Pineda-Mejia, J., Dicke, M., van Loon, J.J.A., 2018b. Performance of the black soldier fly (Diptera: Stratiomyidae) on vegetable residue-based diets formulated based on protein and carbohydrate contents. J. Econ. Entomol. 111, 2676–2683.

Barros, L.M., Gutjahr, A.L.N., Ferreira- Keppler, R.L., Martins, R.T., 2018. Morphological description of the immature stages of *Hermetia illucens* (Linnaeus, 1758) (Diptera: Stratiomyidae). Microsc. Res. Tech. 56, 681–689.

Behmer, S.T., Nes, W.D., 2003. Insect sterol nutrition and physiology: a global overview. Adv. Insect Physiolgy 31, 1–72.

Beniers, J.J.A., Graham, R.I., 2019. Effect of protein and carbohydrate feed concentrations on the growth and composition of black soldier fly (*Hermetia illucens*) larvae. J. Insects as Food Feed 5, 193–199.

Benkel, B.F., Hickey, D.A., 1986. Glucose repression of amylase gene expression in *Drosophila melanogaster*. Genetics 114, 137–144.

Bloukounon-Goubalan, A.Y., Saïdou, A., Chrysostome, C.A.A.M., Kenis, M., Amadji, G. L., Igué, A.M., Mensah, G.A., 2019. Physical and Chemical properties of the agro-processing by-products decomposed by larvae of *Musca domestica* and *Hermetia illucens*. Waste and Biomass Valorization. https://doi.org/10.1007/s12649-019-00587-z.

Bohn, T., Carriere, F., Day, L., Deglaire, A., Egger, L., Freitas, D., Golding, M., Le Feunteun, S., Macierzanka, A., Menard, O., Miralles, B., Moscovici, A., Portmann, R., Recio, I., Rémond, D., Santé-Lhoutelier, V., Wooster, T.J., Lesmes, U., Mackie, A. R., Dupont, D., 2018. Correlation between *in vitro* and *in vivo* data on food digestion. What can we predict with static *in vitro* digestion models?. Crit. Rev. Food Sci. Nutr. 58, 2239–2261.

Boisen, S., Eggum, B.O., 1991. Critical evaluation of *in vitro* methods for estimating digestibility in simple-stomach animals. Nutr. Res. Rev. 4, 141–162.

Boisen, S., Fernández, J.A., 1997. Prediction of the total tract digestibility of energy in feedstuffs and pig diets by *in vitro* analyses. Anim. Feed Sci. Technol. 68, 277–286.

Bonelli, M., Bruno, D., Caccia, S., Sgambetterra, G., Cappellozza, S., Jucker, C., Tettamanti, G., Casartelli, M., 2019. Structural and functional characterization of *Hermetia illucens* larval midgut. Front. Physiol. 10, 204.

Bortolini, S., Macavei, L.I., Saadoun, J.H., Foca, G., Ulrici, A., Bernini, F., Malferrari, D., Setti, L., Ronga, D., Maistrello, L., 2020. *Hermetia illucens* (L.) larvae as chicken manure management tool for circular economy. J. Clean. Prod. https://doi.org/10.1016/j.jclepro.2020.121289.

Brodkorb, A., Egger, L., Alminger, M., Alvito, P., Assunção, R., Ballance, S., Bohn, T., Bourlieu-Lacanal, C., Boutrou, R., Carrière, F., Clemente, A., Corredig, M., Dupont, D., Dufour, C., Edwards, C., Golding, M., Karakaya, S., Kirkhus, B., Le Feunteun, S., Lesmes, U., Macierzanka, A., Mackie, A.R., Martins, C., Marze, S., Mcclements, D. J., Ménard, O., Portmann, R., Santos, C.N., Souchon, I., Singh, R.P., Vegarud, G.E., Wickham, M.S.J., Weitschies, W., Recio, I., 2019. INFOGEST static *in vitro* simulation of gastrointestinal food digestion. Nat. Protoc. 14, 991–1014.

Bruno, D., Bonelli, M., De Filippis, F., Di Lelio, I., Tettamanti, G., Casartelli, M., Ercolini, D., Caccia, S., 2019. The intestinal microbiota of *Hermetia illucens* larvae is affected by diet and shows a diverse composition in the different midgut regions. Appl. Environ. Microbiol. 85, e01864–18.

Bosch, G., Oonincx, D.G.A.B., Jordan, H.R., Zhang, J., van Loon, J.J.A., van Huis, A., Tomberlin, J.K., 2020. Standardisation of quantitative resource conversion studies with black soldier fly larvae. J. Insects as Food Feed 6, 95–109.

Cammack, J., Tomberlin, J.K., 2017. The impact of diet protein and carbohydrate on select life-history traits of the black soldier fly *Hermetia illucens* (L.). (Diptera: Stratiomyidae). Insects 8, 56.

Caccia, S., Casartelli, M., Tettamanti, G., 2019. The amazing complexity of insect midgut cells: types, peculiarities, and functions. Cell and Tissue Research 377, 505–525.

Cappellozza, S., Leonardi, M.G., Savoldelli, S., Carminati, D., Rizzolo, A., Cortellino, G., Terova, G., Moretto, E., Badaile, A., Concheri, G., Saviane, A., Bruno, D., Bonelli, M., Caccia, S., Casartelli, M., Tettamanti, G., 2019. A first attempt to produce proteins from insects by means of a circular economy. Animals 9, 278.

Carvalho, G.B., Kapahi, P., Benzer, S., 2005. Compensatory ingestion upon dietary restriction in *Drosophila melanogaster*. Nat. Methods 2, 813–815.

Chapman, R.F., 2013. The insects: Structure and function. Cambridge University Press, Cambridge, UK.

Cheli, F., Battaglia, D., Pinotti, L., Baldi, A., 2012. State of the art in feedstuff analysis: A technique-oriented perspective. J. Agric. Food Chem. 60, 9529–9542.

Clissold, F.J., Tedder, B.J., Conigrave, A.D., Simpson, S.J., 2010. The gastrointestinal tract as a nutrient-balancing organ. Proc. R. Soc. B Biol. Sci. 277, 1751–1759.

Cohen, A.C., 2005. Insect Diets. CRC Press, Taylor & Francis Group, Broken Sound Parkway NW, USA.

Colombani, J., Raisin, S., Pantalacci, S., Radimerski, T., Montagne, J., Leopold, P., Léopold, P., 2003. A nutrient sensor mechanism controls *Drosophila* growth. Cell 114, 739–749.

Danielsen, E.T., Moeller, M.E., Rewitz, K.F., 2013. Nutrient signalling and developmental timing of maturation. Curr. Top. Dev. Biol. 105, 37–67.

de Carvalho, M.J.M., Mirth, C.K., 2017. Food intake and food choice are altered by the developmental transition at critical weight in *Drosophila melanogaster*. Anim. Behav. 126, 195–208.

De Smet, J., Wynants, E., Cos, P., Van Campenhout, L., 2018. Microbial community dynamics during rearing of black soldier fly larvae (*Hermetia illucens*) and its impact on exploitation potential. Appl. Environ. Microbiol. 85, e02722–17.

Deshpande, S.A., Carvalho, G.B., Amador, A., Phillips, A.M., Hoxha, S., Lizotte, K.J., Ja, W.W., 2014. Quantifying *Drosophila* food intake: Comparative analysis of current methodology. Nat. Methods 11, 535–540.

Dortmans, B., Diener, S., Verstappen, B.M., Zurbrügg, C., 2017. Black soldier fly biowaste processing: A step-by-step guide. Swiss Federal Institute of Aquatic Science and. Technology (Eawag), Dübendorf, Switzerland.

Douglas, A.E., 2010. The Symbiotic Habit. Princeton University Press, Princeton NJ, USA.

Douglas, A.E., 2009. The microbial dimension in insect nutritional ecology. Funct. Ecol. 23, 38–47.

Edgecomb, R.S., Harth, C.E., Schneiderman, A.M., 1994. Regulation of feeding behavior in adult *Drosophila melanogaster* varies with feeding regime and nutritional state. J. Exp. Biol. 197, 215–235.

Ermolaev, E., Lalander, C., Vinnerås, B., 2019. Greenhouse gas emissions from small-scale fly larvae composting with *Hermetia illucens*. Waste Manag. 9, 65–74.

Espinoza-Fuentes, F.P., Terra, W.R., 1987. Physiological adaptations for digesting bacteria - water fluxes and distribution of digestive enzymes in *Musca domestica* larval midgut. Insect Biochem. 17, 809–817.

Fuller, M.F., 1991. *In vitro* digestion for pigs and poultry. C.A.B, International, Wallingford, UK.

Gelperin, A., Dethier, V.G., 1967. Long-term regulation of sugar intake by the blowfly. Physiol. Zool. 40, 218–228.

Gold, M., Cassar, C.M., Zurbrügg, C., Kreuzer, M., Boulos, S., Diener, S., Mathys, A., 2020. Biowaste treatment with black soldier fly larvae: Increasing performance through the formulation of biowastes based on protein and carbohydrates. Waste Manag. 102, 319–329.

Gold, M., Tomberlin, J.J.K., Diener, S., Zurbrügg, C., Mathys, A., 2018a. Decomposition of biowaste macronutrients, microbes, and chemicals in black soldier fly larval treatment: A review. Waste Manag. 82, 302–318.

Gold, M., Spiess, R., Zurbrügg, C., Kreuzer, M., Mathys, A., 2018b. Digestibility of different dietary fibres by black soldier fly larvae. Bornimer Agrartech. Berichte 100, 129–131.

Henningsen, A., Toomet, O., 2011. maxLik: A package for maximum likelihood estimation in R. Comput. Stat. 26, 443–458.

Hur, S.J., Lim, B.O., Decker, E.A., McClements, D.J., 2011. *In vitro* human digestion models for food applications. Food Chem. 125, 1–12.

Jeon, H., Park, S., Choi, J., Jeong, G., Lee, S.B., Choi, Y., Lee, S.J., 2011. The intestinal bacterial community in the food waste-reducing larvae of *Hermetia illucens*. Curr. Microbiol. 62, 1390–1399.

Jiang, S., Teng, C.P., Puah, W.C., Wasser, M., Win, K.Y., Han, M.Y., 2015. Oral Administration and selective uptake of polymeric nanoparticles in *Drosophila* larvae as an *in vivo* model. ACS Biomater. Sci. Eng. 1, 1077–1084.

Karasov, W.H., Martínez del Rio, C., Caviedes-Vidal, E., 2011. Ecological physiology of diet and digestive systems. Annu. Rev. Physiol. 73, 69–93.

Kiers, J.L., Nout, R.M.J., Rombouts, F.M., 2000. *In vitro* digestibility of processed and fermented soya bean, cowpea and maize. J. Sci. Food Agric. 80, 1325–1331.

Kim, G., Huang, J.H., McMullen, J.G., Newell, P.D., Douglas, A.E., 2018. Physiological responses of insects to microbial fermentation products: Insights from the interactions between *Drosophila* and acetic acid. J. Insect Physiol. 106, 13–19.

Lalander, C., Diener, S., Zurbrügg, C., Vinnerås, B., 2019. Effects of feedstock on larval development and process efficiency in waste treatment with black soldier fly (*Hermetia illucens*). J. Clean. Prod. 208, 211–219.

Lam, K., Geisreiter, C., Gries, G., 2009. Ovipositing female house flies provision offspring larvae with bacterial food. Entomol. Exp. Appl. 133, 292–295.

Lee, C.M., Lee, Y.S., Seo, S.H., Yoon, S.H., Kim, S.J., Hahn, B.S., Sim, J.S., Koo, B.S., 2014. Screening and characterization of a novel cellulase gene from the gut microflora of *Hermetia illucens* using metagenomic library. J. Microbiol. Biotechnol. 24, 1196–1206.

Leong, S.Y., Rahman, S., Kutty, M., Malakahmad, A., Tan, C.K., 2016. Feasibility study of biodiesel production using lipids of *Hermetia illucens* larva fed with organic waste. Waste Manag. 47, 84–90.

Leys, C., Ley, C., Klein, O., Bernard, P., Licata, L., 2013. Journal of Experimental Social Psychology Detecting outliers: Do not use standard deviation around the mean, use absolute deviation around the median. Journal of Experimental Social Psychology 4, 764–766.

Matzkin, L.M., Johnson, S., Paight, C., Bozinovic, G., Markow, T.A., 2011. Dietary protein and sugar differentially affect development and metabolic pools in ecologically diverse *Drosophila*. J. Nutr. 141, 1127–1133.

McClements, D.J., Decker, E.A., Park, Y., 2009. Controlling lipid bioavailability through physicochemical and structural approaches. Crit. Rev. Food Sci. Nutr. 49, 48–67.

McDonald, P., Edwards, R.A., Greenhalgh, J.F.D., Morgan, C.A., Sinclair, L.A., Wilkinson, R.G., Edwards, M., Morgan, G., Wilkinson, S., 2011. Animal nutrition. Prentice Hall, Harlow, England.

Merali, Z., Collins, S.R.A., Elliston, A., Wilson, D.R., Käsper, A., Waldron, K.W., 2015. Characterization of cell wall components of wheat bran following hydrothermal pretreatment and fractionation. Biotechnol. Biofuels 8, 1–13.

Mertenat, A., Diener, S., Zurbrügg, C., 2019. Black Soldier Fly biowaste treatment – Assessment of global warming potential. Waste Manag. 84, 173–181.

Miguel-Aliaga, I., Jasper, H., Lemaitre, B., 2018. Anatomy and physiology of the digestive tract of *Drosophila melanogaster*. Genetics 210, 357–396.

Minekus, M., Alminger, M., Alvito, P., Ballance, S., Bohn, T., Bourlieu, C., Carrière, F., Boutrou, R., Corredig, M., Dupont, D., Dufour, C., Egger, L., Golding, M., Karakaya, S., Kirkhus, B., Le Feunteun, S., Lesmes, U., Macierzanka, A., Mackie, A., Marze, S., McClements, D.J., Ménard, O., Recio, I., Santos, C.N., Singh, R.P., Vegarud, G.E., Wickham, M.S.J., Weitschies, W., Brodkorb, A., 2014. A standardised static *in vitro* digestion method suitable for food – an international consensus. Food Funct. 5, 1113–1124.

Mumcuoglu, K.Y., Miller, J., Mumcuoglu, M., Friger, M., Tarshis, M., 2001. Destruction of bacteria in the digestive tract of the maggot of *Lucilia sericata* (Diptera: Calliphoridae). J. Med. Entomol. 38, 161–166.

Musselman, L.P., Fink, J.L., Narzinski, K., Ramachandran, P.V., Hathiramani, S.S., Cagan, R.L., Baranski, T.J., 2011. A high-sugar diet produces obesity and insulin resistance in wild-type *Drosophila*. DMM Dis. Model. Mech. 4, 842–849.

Noblet, J., Jaguelin-Peyraud, Y., 2007. Prediction of digestibility of organic matter and energy in the growing pig from an *in vitro* method. Anim. Feed Sci. Technol. 134, 211–222.

Oomen, A.G., Hack, A., Minekus, M., Zeijdner, E., Cornelis, C., Schoeters, G., Verstraete, W., Van De Wiele, T., Wragg, J., Rompelberg, C.J.M., Sips, A.J.A.M., Van Wijnen, J.H., 2002. Comparison of five *in vitro* digestion models to study the bioaccessibility of soil contaminants. Environ. Sci. Technol. 36, 3326–3334.

Oomen, A.G., Rompelberg, C.J.M., Bruil, M.A., Dobbe, C.J.G., Pereboom, D.P.K.H., Sips, A.J.A.M., 2003. Development of an *in vitro* digestion model for estimating the bioaccessibility of soil contaminants. Arch. Environ. Contam. Toxicol. 44, 281–287.

Pang, W., Hou, D., Chen, J., Nowar, E.E., Li, Z., Hu, R., Tomberlin, J.K., Yu, Z., Li, Q., Wang, S., 2020. Reducing greenhouse gas emissions and enhancing carbon and nitrogen conversion in food wastes by the black soldier fly. Journal of Environmental Management 260. https://doi.org/10.1016/j.jenvman.2020.110066.

R Core Team, 2017. R: A language and environment for statistical computing [WWW Document]. URL https://www.r-project.org/.

Rehman, K. ur, Rehman, A., Cai, M., Zheng, L., Xiao, X., Somroo, A.A., Wang, H., Li, W., Yu, Z., Zhang, J., 2017. Conversion of mixtures of dairy manure and soybean curd residue by black soldier fly larvae (*Hermetia illucens* L.). J. Clean. Prod. 154, 366–373.

Rodrigues, M.A., Martins, N.E., Balancé, L.F., Broom, L.N., Dias, A.J.S., Fernandes, A.S. D., Rodrigues, F., Sucena, É., Mirth, C.K., 2015. *Drosophila melanogaster* larvae make nutritional choices that minimize developmental time. J. Insect Physiol. 81, 69–80.

Romero, A., Broce, A., Zurek, L., 2006. Role of bacteria in the oviposition behaviour and larval development of stable flies. Med. Vet. Entomol. 20, 115–121.

Sakaguchi, H., Suzuki, M.G., 2013. *Drosophila melanogaster* larvae control amylase secretion according to the hardness of food. Front. Physiol. 4, 200.

Smetana, S., Palanisamy, M., Mathys, A., Heinz, V., 2016. Sustainability of insect use for feed and food: Life Cycle Assessment perspective. J. Clean. Prod. 137, 741–751.

Smetana, S., Schmitt, E., Mathys, A., 2019. Sustainable use of *Hermetia illucens* insect biomass for feed and food: Attributional and consequential life cycle assessment. Resour. Conserv. Recycl. 144, 285–296.

Setti, L., Francia, E., Pulvirenti, A., Gigliano, S., Zaccardelli, M., Pane, C., Caradonia, F., Bortolini, S., Maistrello, L., Ronga, D., 2019. Use of black soldier fly (*Hermetia illucens* (L.), Diptera: Stratiomyidae) larvae processing residue in peat-based growing media. Waste Manag. 95, 278–288.

Simpson, S.J., Browne, L.B., van Gerwen, A.C.M., 1989. The patterning of compensatory sugar feeding in the Australian sheep blowfly. Physiol. Entomol. 14, 91–105.

Stana-Kleinschek, K., Ribitsch, V., Kreze, T., Fras, L., 2002. Determination of the adsorption character of cellulose fibres using surface tension and surface charge. Mater. Res. Innov. 6, 13–18.

Storelli, G., Defaye, A., Erkosar, B., Hols, P., Royet, J., Leulier, F., 2011. *Lactobacillus plantarum* promotes *Drosophila* systemic growth by modulating hormonal signals through TOR-dependent nutrient sensing. Cell Metab. 14, 403–414.

Terra, W.R., Ferreira, C., 2012. Biochemistry and molecular biology of digestion, in: Insect molecular biology and biochemistry. Academic Press, 365–418.

Tilley, J.M.A., Terry, R.A., 1963. A two stage technique for *in vitro* digestion of forage crops. J. Br. Grassl. Soc. 18, 104–111.

Van Soest, P.J., 1994. Nutritional ecology of ruminants. Cornell University Press, Ithaca NY, USA.

Vilcinskas, A., 2013. Yellow Biotechnology I: Insect Biotechnologie in Drug Discovery and Preclinical Research. Springer, Berlin, Germany.

Wahlgren, M., Axenstrand, M., Håkansson, Å., Marefati, A., Pedersen, B.L., 2019. *In vitro* methods to study colon release: State of the art and an outlook on new strategies for better *in-vitro* biorelevant release media. Pharmaceutics 11, 95.
Wang, Y.-S., Shelomi, M., 2017. Review of black soldier fly (*Hermetia illucens*) as animal feed and human food. Foods 6, 91.
Waterhouse, D.F., 1954. The rate of the production of the peritrophic membrane in some insects. Aust. J. Biol. Sci. 7, 59–72.
Wetzel, R.G., Likens, G.E., 2000. Limnological Analyses. Springer Science & Business Media, Berlin, Germany.
Wong, A.C.-N., Dobson, A.J., Douglas, A.E., 2014. Gut microbiota dictates the metabolic response of *Drosophila* to diet. J. Exp. Biol. 217, 1894–1901.
Zhao, Y., Wang, W., Zhu, F., Wang, Xiaoyun, Wang, Xiaoping, Lei, C., 2017. The gut microbiota in larvae of the housefly *Musca domestica* and their horizontal transfer through feeding. AMB Express 7, 147.
Zanotto, F.P., Simpson, S.J., Raubenheimer, D., 1993. The regulation of growth by locusts through post-ingestive compensation for variation in the levels of dietary protein and carbohydrate. Physiological Entomology 18, 425–434.